

Structure sensitivity and kinetics of D-glucose oxidation to D-gluconic acid over carbon-supported gold catalysts

Y. Önal, S. Schimpf, and P. Claus*

Department of Chemistry, Chemical Technology II, Darmstadt University of Technology, Petersenstrasse 20, D-64287 Darmstadt, Germany

Received 10 October 2003; revised 6 January 2004; accepted 6 January 2004

Abstract

The heterogeneously catalyzed oxidation of D-glucose to D-gluconic acid over Au/C catalysts has been studied. A series of Au/C catalysts were prepared by the gold sol method with different reducing agents and different kinds of carbon support providing Au mean particle diameters in the range 3–6 nm. The activities of these catalysts with respect to D-glucose oxidation were compared, and several aspects influencing activity, especially Au particle size, were discussed. The influence of reaction conditions ($T = 30\text{--}90\text{ }^{\circ}\text{C}$, pH 7.0–9.5) on the kinetics of the D-glucose oxidation has been examined using the most active Au/C catalyst. By a detailed analysis of all reaction products under different reaction conditions, a reaction network of the D-glucose oxidation is presented, and a reaction mechanism for D-glucose oxidation that explains the influence of pH on reaction rate is proposed. Ensuring that D-glucose oxidation takes place in the kinetic regime (sufficient stirring rate and airflow rate), a semiempirical model based on a Langmuir–Hinshelwood-type reaction pathway is assumed. At $50\text{ }^{\circ}\text{C}$ and pH 9.5 kinetic parameters were calculated by an optimization routine. The resulting concentration courses of D-glucose and D-gluconic acid were in good agreement with the experimental data. All experiments were carried out in a semibatch reactor under pH control at atmospheric pressure.

© 2004 Elsevier Inc. All rights reserved.

Keywords: D-Glucose oxidation; Au/C catalysts; Structure sensitivity; Specific gold surface area; Gold nanoparticle; Gold sol method; Mass transfer; Langmuir–Hinshelwood kinetics

1. Introduction

D-Gluconic acid is an important intermediate in the field of food industry and pharmaceutical applications and is usually produced by enzymatic oxidation of D-glucose [1] with an estimated market of 60,000 tons per year [2]. Besides this route, recent developments have shown the potential of heterogeneous catalysts for oxidizing glucose with oxygen or air. Most of the catalysts are based on supported platinum group metals, and various factors controlling activity and selectivity were studied. The main disadvantage is deactivation of the catalysts with increasing reaction time, i.e., with conversion. Improvement of activity/selectivity and stability can be achieved in the presence of a second metal in ex situ-prepared bimetallic catalysts (especially bismuth as promotor) [3] and by the nature of the individual metal [4]. With respect to the latter, gold on activated charcoal [5]

or on oxides [6] is the preferred catalyst for the oxidation of functional groups ($-\text{OH}$, $\text{C}=\text{O}$). Even when their mean gold particle sizes were similar, carbon proved to be more advantageous as a support than oxidic materials in the liquid-phase oxidation of alcohols and aldehydes. The gold sol method is an easy and effective way of preparing highly active carbon-supported Au catalysts with small gold particle diameters (4–9 nm) [7–9]. The particle diameter can thereby be easily influenced by variation of certain preparation parameters (reduction agent, concentrations of reagents [8], temperature [10]). By use of this preparation method, Au/C-catalyzed oxidation of D-glucose to D-gluconic acid in the aqueous phase has already been examined by Prati et al. [5]. In particular, the influence of pH value on reaction rate was studied in comparison with other catalysts based on Pt group metals. Au/C was found to be the most active catalyst independent of pH value, and it could be shown that the activity of the Au/C catalyst was less sensitive to lower pH values.

With respect to our research program on the catalytic chemistry of renewable resources including the oxida-

* Corresponding author.

E-mail address: claus@ct.chemie.tu-darmstadt.de (P. Claus).

tion [11] and hydrogenation of sugars [12] and stimulated by the promising results of liquid-phase oxidation using gold catalysts [5], we report first in this article the characterization of carbon-supported gold catalysts by transmission electron microscopy (TEM) and X-ray photoelectron spectroscopy (XPS) with the aim of studying the influence of gold particle size and surface composition on activity and selectivity (structure sensitivity) of glucose oxidation over gold catalysts. Then, we focus on the kinetics under optimized reaction conditions (pH 9.5, $T = 50^\circ\text{C}$) which has never been investigated before. For this purpose, Au/C catalysts with different mean Au particle diameters were prepared by the gold sol method using different reducing agents (NaBH_4 and tetrahydroxymethylphosphonium chloride, THPC) and carbon supports. The kinetics of glucose oxidation was estimated by appropriate experiments with the most active Au/C catalyst at different glucose and catalyst concentrations in the kinetic regime at 50°C and pH 9.5. Parameters of the semiempirical reaction rate, which was proposed assuming a Langmuir–Hinshelwood model, were calculated by an optimization routine.

2. Experimental

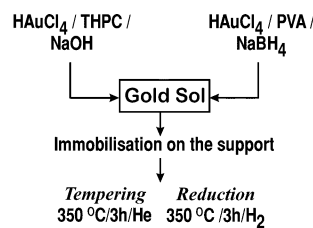
2.1. Catalyst preparation

2.1.1. Reagents

THPC (78 wt%), polyvinyl alcohol (PVA) (> 98%), and NaOH (0.2 M) were purchased from Merck and $\text{HAuCl}_4 \cdot 3\text{H}_2\text{O}$ (99.99% ACS, Au 49.5% min.) from Alfa Aesar. Two types of carbon supports were used, namely, Black Pearls 2000 (GP3755) and Vulcan XC72R (GP3759), which were kindly listed by CABOT GmbH. Characteristic support data are listed in Table 1.

2.1.2. Preparation procedure

Au/C catalysts were prepared by the gold sol method with two different types of reducing agents, NaBH_4 and THPC, which lead to small Au particle sizes as reported in [7–10]. Depending on the reduction agent used, the preparation methods are slightly different as described in the literature. The principle of the preparation procedures described below



Scheme 1. Overview of the preparation/activation procedure.

is illustrated in Scheme 1. The amounts of the reagents given in the text were calculated in order to prepare 5 g Au/C catalyst with an Au loading of 1 wt%.

2.1.2.1. THPC/NaOH method H_2O (232 mL) was first mixed with (0.2 M) NaOH (7.5 mL), and afterward 5 mL THPC (1.2 mL of the 78 wt% THPC solution was diluted with water to 100 mL) was added into the alkaline solution while the mixture was stirred. After 2 more min of stirring, 6 mL HAuCl_4 (0.043 M) was introduced into the solution. Formation of the gold sol (brown color of solution) occurred immediately. Then, 5 g carbon was suspended in 500 mL H_2O and agitated for 15 min in an ultrasonic bath. The gold sol was then added to the support suspension.

2.1.2.2. PVA/ NaBH_4 method HAuCl_4 (0.0877 g, 258 mmol) was dissolved in 1.725 L H_2O and then, while the mixture was stirred, mixed with 4 mL PVA solution (2 wt%). Afterward, 10 mL NaBH_4 (0.1 M) was dropped into the mixture. Again, the formation of the gold sol occurred immediately. Then 5 g carbon was added to the gold sol.

Both with the THPC/NaOH method and the NaBH_4 /PVA method, immobilization of the gold sol on the support was completed after 1–3 days. During this time the gold sol became colorless. The adsorbed support was then filtered, washed with water to free the filtrate of chloride (AgNO_3 test), dried, and mortared. The organic scaffold was removed from the support by inert gas treatment (3 h/ $350^\circ\text{C}/\text{He}$). The catalysts were activated by a reducing process (3 h/ $350^\circ\text{C}/\text{H}_2$).

2.2. Catalyst characterization

The metal content of the Au/C catalysts was determined by optical emission spectroscopy with inductive coupled plasma (ICP-OES). For this purpose the samples were solubilized in aqua regia (HCl/HNO_3).

Mean particle diameters of the gold on the carbon support were determined by TEM analysis. The samples were dispersed in isopropanol, agitated in an ultrasonic bath, and deposited on a commercially available Cu support net (grid 300, Plano). Particle size of the reduced samples was examined in the light- and darkfield modes in association with selected area electron diffraction (SAED) with a JEM 100C (100 kV). Mean particle diameters were calculated on the assumption of a logarithmic normal distribution of the particle sizes.

Table 1
Characteristic data of the carbon supports used^a

Property	Black Pearls 2000 GP3755	Vulcan XC72R GP3759
Specific surface area (m^2/g)	1635	245
Micropore volume (mL/g)	0.59	0.06
Iodine number (mg/g)	1400	253
Total sulfur (%)	1.0	0.5
pH	9.5	6.0
+325 mesh residue [max ppm]	200	25
Density (g/L)	150	270

^a Data from manufacturer [23].

X-Ray photoelectron spectra were obtained with a VG ESCALAB 220 iXL equipped with a monochromated Al-K α radiation source (1486.6 eV) and pass energies of 150 eV (overview spectra) and 25 eV (high-resolution mode). Details of both the procedure applied to the gold catalysts and the data evaluation were published recently [13]. Peak positions could be determined with a precision of ± 0.1 eV. Gold catalysts were analyzed as prepared and after two different pretreatment procedures, i.e., heating in flowing argon and hydrogen at 350 °C. This pretreatment was carried out in a gas cell integrated into the lock of the system at the desired temperature and in the gas flux. Thus, it was possible to transfer the sample from this gas cell to the UHV analysis chamber without air contact. The pressure in the analysis chamber was below 1×10^{-6} Pa.

2.3. Liquid-phase oxidation of glucose

Catalytic runs were carried out in a 250-mL five-necked glass reactor. The reactor was equipped with several inlets and detectors to monitor the reaction conditions. During the experiment, the temperature of the three-phase reaction mixture and the pH value (pH electrode from HANNA Instruments), which also depends on temperature, were indicated. By a drop funnel filled with NaOH solution (4 wt%), the pH value could be maintained at a certain value. Air was bubbled through the reaction mixture at a constant flow rate at atmospheric pressure. The reactor was additionally equipped with a cooler, so that any evaporation of the liquid phase could be neglected. A hotplate equipped with a stirrer provided the heat needed to achieve the desired reaction temperature and an intensive mixing of the reaction mixture.

A typical catalytic run was carried out with 100 mL D-glucose solution (4 wt%) and 432 mg Au/C catalyst (molar ratio of D-glucose to Au: 1000). Both the catalyst and the D-glucose solution were first mixed together, and at a low stirring rate the mixture was heated to the desired temperature. The reaction was started by accelerating the stirring rate, switching on the air supply, and adjusting to a certain pH value by dropping an adequate amount of NaOH solution. During the whole reaction, pH was kept at the desired value by continuous NaOH drop. The products of the reaction mixture at different reaction periods were quantitatively analyzed by HPLC (Bio-Rad, Aminex HPX-87H). The reaction was complete when there was no significant change of pH value.

3. Results

3.1. Catalyst characterization

Gold content of the prepared Au/C catalysts is summarized in Table 2. According to the ICP-OES analysis, the amount of gold on each support, independent of the preparation method, was less than 1 wt% (0.42–0.70 wt%). The

Table 2

Au content of the prepared Au/C catalysts resulting from ICP-OES analysis

Catalyst	Au content (wt%)
Au/C GP3755 PVA	0.60
Au/C GP3759 PVA	0.42
Au/C GP3755 THPC	0.70
Au/C GP3759 THPC	0.48

discrepancy between the calculated and analyzed Au content can be explained by a nonquantitative immobilization of the gold sol on the support, probably depending on the microstructure and chemical composition of the carbon varying both the distribution of the gold particles and their interaction with the support.

TEM images of the catalyst surface are shown in Fig. 1 together with the average gold particle diameter and its standard deviation. The catalysts contain nanosized gold particles in the range 3 to 6 nm. By variation of the preparation method (PVA/NaBH $_4$ vs THPC/NaOH, see Section 2.1.2) and use of the same support (GP3755 or GP3759), gold particle diameter decreases as shown in Fig. 1 by comparing the upper and lower TEM images. A more striking decrease in gold particle size was observed when only the carbon support was varied for the same preparation method applied (compare left- and right-hand side images in Fig. 1). Generally, the results of TEM analysis clearly show that the mean Au particle size is considerably smaller on the carbon support GP3759 (Vulcan) than on GP3755 (Black Pearls), independent of the catalyst preparation method applied.

Whereas the characterization of oxide-supported gold catalysts by X-ray photoelectron spectroscopy exhibited pronounced shifts in Au 4f $_{7/2}$ binding energy to lower values [13] compared with the binding energy of metallic gold (84.2 eV [14]), XPS measurements on the carbon-supported gold catalysts in this study gave an average value of 84.15 ± 0.05 eV for binding energy, independent of the pretreatment method applied. This corresponds to the value of metallic gold.

3.2. Optimization of the reaction conditions

3.2.1. Reaction temperature

The influence of reaction temperature (other reaction conditions remained constant) on the reaction rate of D-glucose oxidation was estimated at an alkaline (pH 9.5) as well as neutral (pH 7.0) pH value. The catalyst used was Au/C GP 3759 THPC, which had proved to be particularly active in previous experiments. The initial reaction rates of D-gluconic acid formation at different reaction temperatures and pH values are depicted in Fig. 2. An optimal temperature range was found at which the reaction rate increased as high as possible. This range is around 50 °C at pH 9.5 and 60 °C at pH 7.0. The decrease in reaction rate of D-gluconic acid formation at higher temperatures can be explained by the side reactions of D-glucose in the aqueous phase which

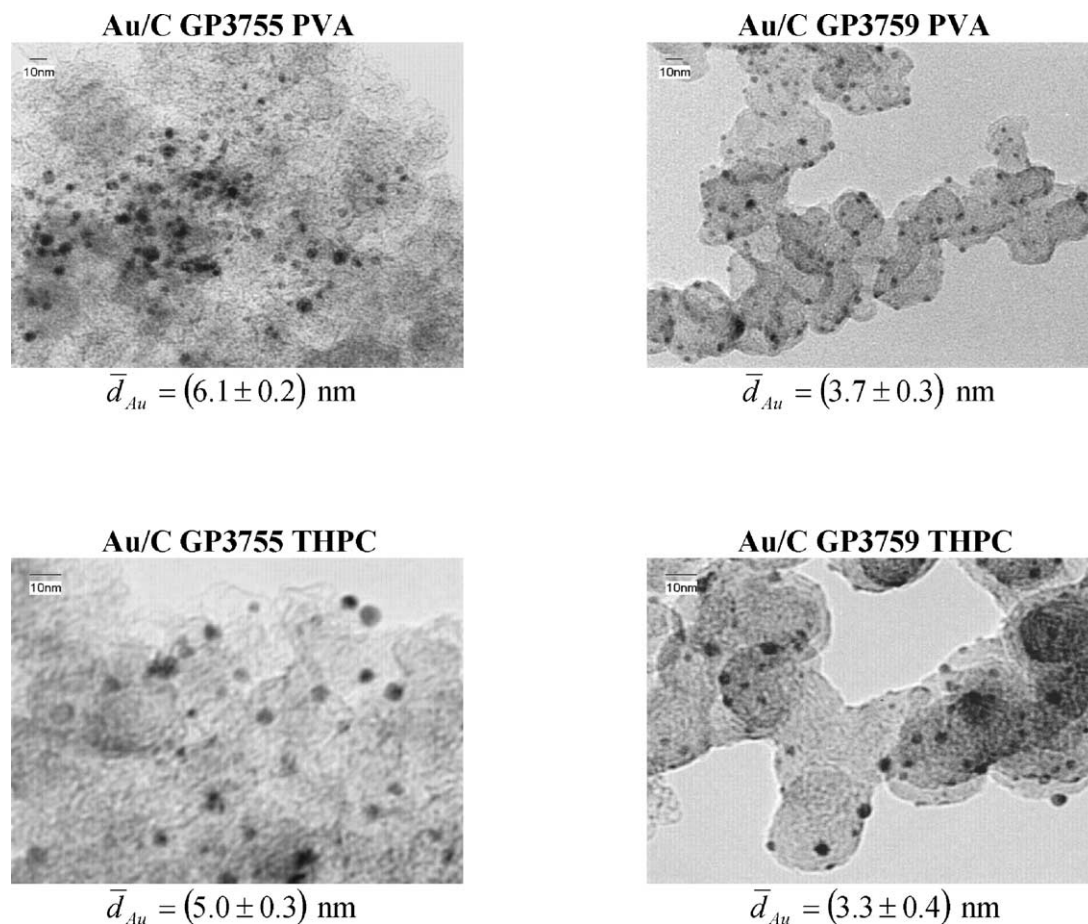


Fig. 1. TEM images and mean gold particle diameters.

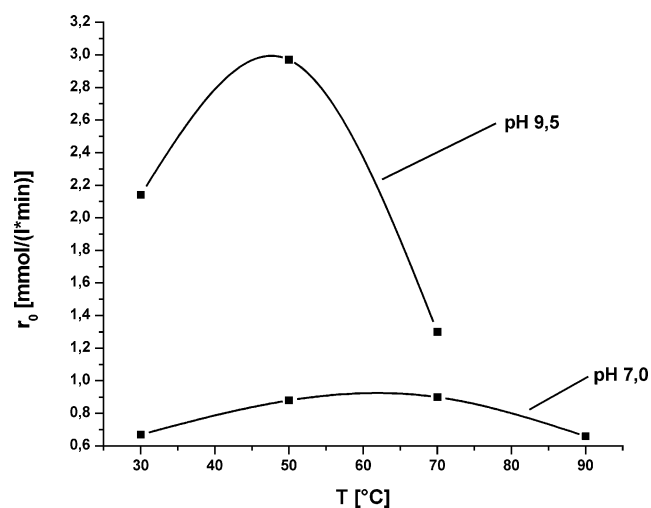
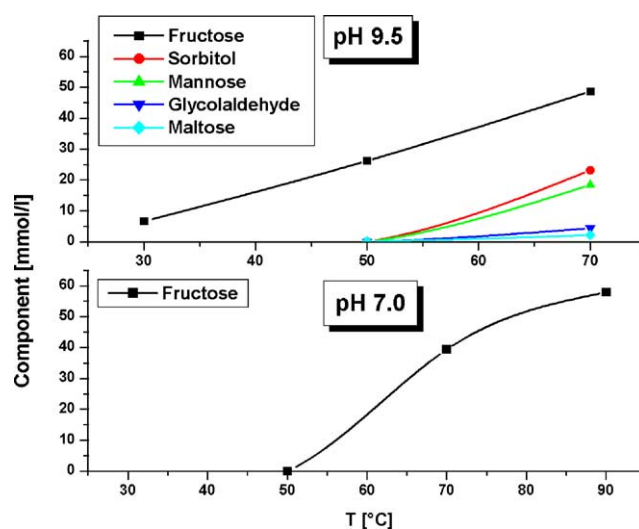


Fig. 2. Initial reaction rates of D-gluconic acid formation at different reaction temperatures and pH values (catalyst: Au/C GP3759 THPC).

Fig. 3. Formation of by-products at pH 7.0 ($t = 300 \text{ min}$) and pH 9.5 ($t = 60 \text{ min}$) as a function of reaction temperature (catalyst: Au/C GP3759 THPC).

are favored at higher temperatures and pH values, as shown in Fig. 3. Therefore, significant by-products of D-glucose oxidation are fructose, mannose, glycolaldehyde, sorbitol, and maltose as described in the reaction network of glucose oxidation given in Section 4.3 (cf. Fig. 11). The decrease in

selectivity to D-gluconic acid with increasing temperature is shown in Fig. 4. At alkaline pH values, the degree of dependency of the reaction rate and selectivity to D-gluconic acid on temperature is higher than at lower pH values.

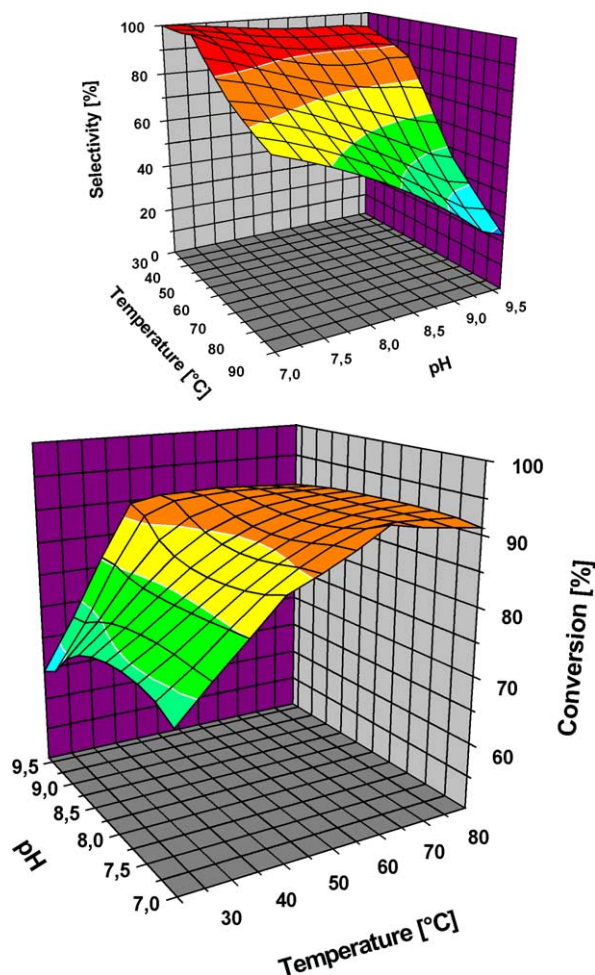


Fig. 4. Selectivity to D-gluconic acid (top) and conversion of glucose (bottom) at different pH and temperature values (catalyst: Au/C GP3759 THPC).

3.2.2. pH value

Au catalysts are less sensitive to lower pH values with respect to their activity in the oxidation of D-glucose than catalysts based on Pd group metals according to [5]. As shown in Fig. 2, the reaction rate of D-gluconic acid formation could be strongly increased at alkaline pH values. By increasing the pH value of the reaction mixture from 7.0 to 9.5 ($T = 50^\circ\text{C}$), the initial reaction rate of D-gluconic acid formation could be accelerated by a factor of 3.2. An important drawback of this phenomenon is the decrease in selectivity to D-gluconic acid at higher pH values (Fig. 4), mainly by isomerization of D-glucose to fructose. However, in contrast to the results presented in [5], the activity of Au/C catalysts in the present study exhibited significant dependence on the pH value.

3.3. Influence of the Au particle diameter on the catalytic activity

Catalytic activity of catalysts with different mean Au particle diameters (Fig. 1) was examined with respect to

Table 3

Calculated Au specific surface areas of different catalysts based on ICP-OES and TEM results

Catalyst	A_{spec} (m^2/g)
Au/C GP 3755 PVA	51.0
Au/C GP 3759 PVA	84.0
Au/C GP 3755 THPC	62.2
Au/C GP 3759 THPC	94.2

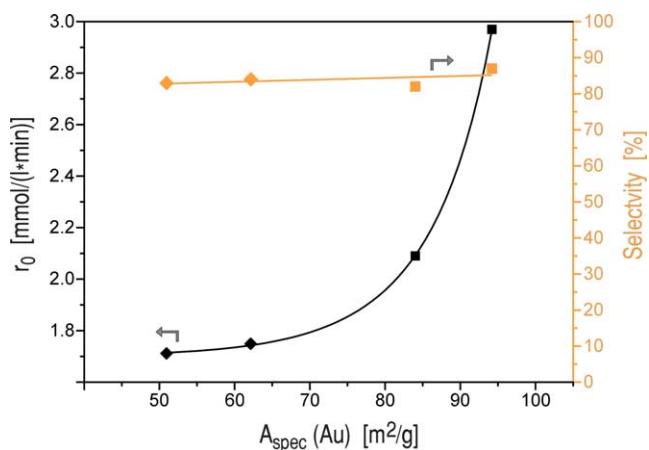


Fig. 5. Initial reaction rates of D-gluconic acid formation and selectivities to D-gluconic acid (pH 9.5 and $T = 50^\circ\text{C}$), as a function of specific Au surface area: \blacklozenge , GP3755; \blacksquare , GP3759.

D-glucose oxidation at 50°C and pH 9.5, as these values represent the optimized reaction conditions with respect to reaction rate and selectivity as presented above. The goal was to find a correlation between catalytic activity and Au particle diameter which has not been investigated so far.

Because the Au contents of the catalysts differ widely (Table 2), catalytic activity could not be correlated only with Au mean particle diameter. Therefore, specific surface area (A_{spec}) of the active component of each catalyst was calculated based on the results of ICP-OES and TEM analysis by assuming closed-shell gold particles of nearly spherical shape [15] (Table 3). As the distribution of the particle diameter of each catalyst was nearly symmetric, mean particle diameters were used to calculate the specific surface areas. Initial reaction rates of D-gluconic acid formation and selectivities to D-gluconic acid as a function of specific surface area are illustrated in Fig. 5. In the field examined, catalytic activity correlates exponentially with specific surface area, whereas selectivity to D-gluconic acid does not change with increasing specific surface area. According to the results presented, there must be a particle size effect of Au/C catalysts in the aqueous-phase oxidation of D-glucose to D-gluconic acid and, thus, the structure sensitivity of the reaction is satisfactorily shown.

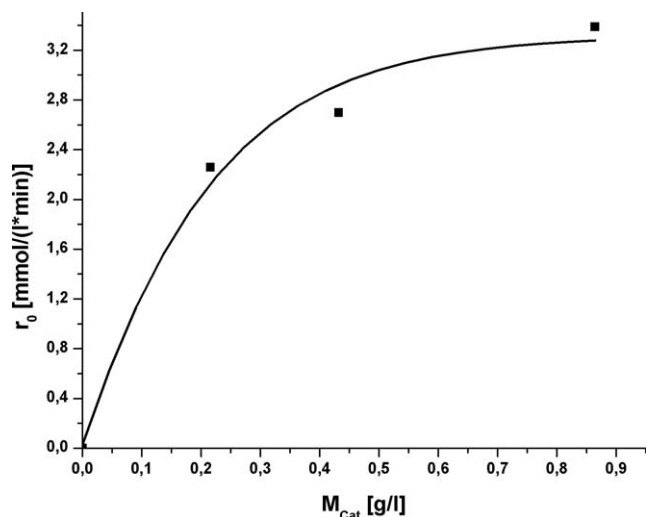


Fig. 6. Initial reaction rates of D-gluconic acid formation at different catalyst concentrations ($T = 50^\circ\text{C}$, pH 9.5, catalyst: Au/C GP3759 THPC).

3.4. Kinetics

3.4.1. Influence of catalyst concentration and D-glucose concentration on reaction rate

To ensure that the reaction rate is not limited by mass transfer at the phase boundaries, the effects of stirring rate as well as airflow rate on reaction rate were examined at 50°C and pH 9.5. It was found that at stirring rates higher than 900 rpm and airflow rates higher than 1600 mL/min, the overall reaction rate is not limited by external mass transfer (diffusion). Kinetic measurements with varied catalyst and D-glucose concentrations were therefore carried out at a stirring rate of 900 rpm and an airflow rate of 2000 mL/min. The influence of catalyst concentration on the reaction rate of D-gluconic acid formation at 50°C and pH 9.5 with the Au/C GP3759 THPC catalyst is presented in Fig. 6, which demonstrates the asymptotic dependence of reaction rate on catalyst concentration.

Initial reaction rates of D-gluconic acid formation and selectivities to D-gluconic acid at different initial D-glucose concentrations are shown in Fig. 7. Obviously the dependence of reaction rate on initial D-glucose concentration is negligible. If the overall reaction rate of D-glucose oxidation was limited by adsorption of D-glucose on the catalyst surface, the reaction rate should show a strong increase with increasing initial D-glucose concentration. According to the results presented here, the overall reaction rate is limited by the surface reaction or the desorption of D-gluconic acid. As the isomerization of D-glucose to fructose increases with increasing initial D-glucose concentration, the selectivity to D-gluconic acid slightly decreases.

3.4.2. Kinetic model

Oxidation of D-glucose in the aqueous phase over Au/C catalysts with oxygen can be described by a Langmuir–Hinshelwood-type model which is schematically represented by the catalytic cycle shown in Fig. 8. The oxida-

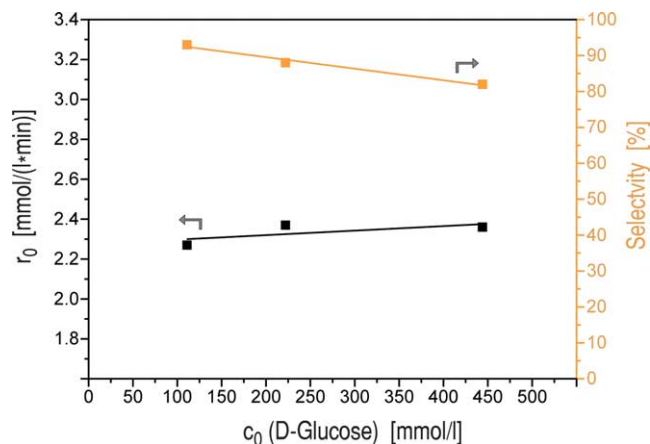


Fig. 7. Initial reaction rates of D-gluconic acid formation and selectivities to D-gluconic acid ($t = 30$ min) at different initial D-glucose concentrations ($T = 50^\circ\text{C}$, pH 9.5, catalyst: Au/C GP3759 THPC).

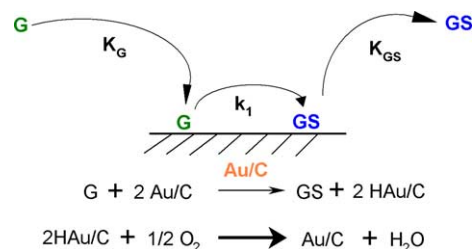


Fig. 8. D-Glucose oxidation over Au according to the Langmuir–Hinshelwood model.

tive dehydrogenation mechanism commonly passed in the liquid-phase oxidation of alcohols and aldehydes is well established in the literature [16] and was also adopted in the oxidation of D-glucose. Sorption of the D-glucose hydrate on the catalyst surface is represented by the sorption constant K_G , whereas k_1 is the rate constant for the dehydrogenation reaction on the catalyst surface and K_{GS} is the sorption constant of D-gluconic acid. Hydrides bound to the catalyst surface as a consequence of dehydrogenation of the substrate subsequently react with dissociatively adsorbed oxygen to form water, which is desorbed. The oxidation reaction of the hydrides should be fast compared with the dehydrogenation reaction. Thus, the whole reaction mechanism can be reduced to three elementary reactions, namely, adsorption of D-glucose, surface reaction of D-glucose, and desorption of gluconic acid.

According to the results presented in Section 3.4.1, it was ruled out that the reaction is limited by adsorption of D-glucose on the catalyst surface. As all kinetic experiments were performed in an alkaline medium, the desorption of gluconic acid should also be faster than the surface reaction [10,17]. Thus, it can be concluded that the surface reaction is the rate-determining step of the overall reaction and is expressed in the equation

$$r_{\text{surface}} = r_{\text{OR}} = k_1 \theta_G - k_{-1} \theta_{\text{GS}}. \quad (1)$$

Consequently, the other elementary steps are in equilibrium,

$$r_{\text{Sor,G}} = r_{\text{Sor,GS}} = 0, \quad (2)$$

and the overall reaction rate of D-gluconic acid formation can be expressed as

$$r_{\text{OR}} = \frac{d[\text{GS}]}{dt} = \frac{k_1 K_G [\text{G}]}{1 + K_G [\text{G}] + K_{\text{GS}} [\text{GS}]} \cdot M_C. \quad (3)$$

Because the rate of conversion of D-glucose is faster than the rate of formation of D-gluconic acid due to additional side reactions, the latter were considered by a further kinetic term in the overall reaction rate of D-glucose consumption:

$$-\frac{d[\text{G}]}{dt} = \frac{K_G k_1 [\text{G}]}{1 + K_G [\text{G}] + K_{\text{GS}} [\text{GS}]} \cdot M_C + k_p [\text{G}]. \quad (4)$$

Taking the selectivity of the reaction at 50 °C and pH 9.5 and already calculated values of kinetic parameters for D-glucose oxidation over Pd/Al₂O₃ catalysts [18] (Table 4) into account, the empirical constant k_p was suggested to be $6 \times 10^{-5} \text{ s}^{-1}$. The product of K_G and k_1 was expressed as k_{Ox} in the program code for the optimization routine. Initial values for the parameter optimization are from the literature [18]. Fig. 9 presents the kinetic parameters determined and the concentration courses of D-glucose and D-gluconic acid calculated, which are in good agreement with the experimental data obtained at 50 °C and pH 9.5 with the Au/C GP3759 THPC catalyst.

Table 4
Kinetic parameters of D-glucose oxidation over Pd/Al₂O₃ catalysts at 50 °C and pH 9 [18]

$k_{\text{Ox}} = 7.9 \times 10^{-4} \text{ L g}^{-1} \text{ s}^{-1}$
$K_G = 138.0 \times 10^{-4} \text{ L mmol}^{-1}$
$K_{\text{GS}} = 279.0 \times 10^{-4} \text{ L mmol}^{-1}$

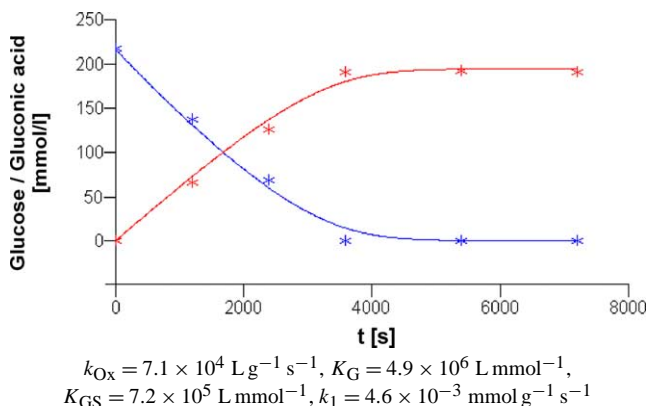


Fig. 9. Comparison of calculated (—) and experimental (*) concentrations versus time of D-glucose and D-gluconic acid ($T = 50^\circ\text{C}$, pH 9.5, catalyst: Au/C GP3759 THPC) and kinetic parameters.

4. Discussion

4.1. Influence of reaction conditions on kinetics

The effect of temperature on reaction rate and selectivity to D-gluconic acid was examined with the catalyst Au/C GP3759 THPC at pH 7.0 as well as at pH 9.5. In both cases, the highest reaction rates were obtained in the temperature regime 50 to 60 °C, while the temperature has a more important effect on the reaction rate at higher pH values. According to ICP-OES analysis of the product solutions obtained after glucose oxidation, Au leaching could be neglected within the detection limit of the method applied ($< 2 \text{ mg/L}$) at any reaction temperature. Thus, a decrease in activity caused by catalyst deactivation, i.e., by loss of metal, with increasing reaction temperature can be excluded. In the literature [5], analysis of fresh and used catalysts revealed leaching of gold when the oxidation was carried out at pH 7, whereas no leaching was observed at pH 9.5. In the present study, however, no correlation of the dependence of the reaction rate on pH value with Au leaching could be found based on ICP-OES analysis. The temperature effect can be explained by the following phenomena. At both pH 7.0 and pH 9.5, selectivity to D-gluconic acid decreases with increasing temperature due to side reactions, as discussed in Section 3.2.1. Moreover, another aspect that has to be taken into account is the solubility of oxygen in water, which decreases with increasing temperature [19]. Thus, the concentration of oxygen in the aqueous phase should limit the overall reaction rate of D-glucose oxidation at higher reaction temperatures. On the other hand, at lower temperatures, the reaction is limited by kinetics as shown in Fig. 2.

The pH value of the reaction mixture has a crucial effect on the reaction rate of D-gluconic acid formation. The reaction rate clearly accelerates with increasing pH value. A possible explanation for this phenomenon is the neglect of catalyst deactivation by self-poisoning in alkaline solution, as D-gluconic acid is then deprotonated and, thus, no longer capable of blocking active centers on the catalyst surface [3,4,17]. Fig. 10 illustrates the concentration courses of D-gluconic acid and temporal reaction rates of D-gluconic acid formation at 50 °C and pH 7.0 or 9.5, respectively. After certain reaction periods which correspond to the same conversion degrees at different reaction conditions, the decrease in reaction rate at pH 7.0 was greater than at pH 9.5, namely, by a factor of nearly 2. Thus, significant catalyst deactivation by self-poisoning should be taken into account when the reaction is not performed in an alkaline reaction medium. On the other hand, selectivity to D-gluconic acid decreases at higher pH values (≥ 9.5) as a result of isomerization and irreversible by-product formation catalyzed in alkaline solutions (Fig. 11).

If, however, only self-poisoning was responsible for the different catalytic activities at different pH values, reaction rates at the beginning of each experiment should be at least similar without consideration of the pH value, because at the

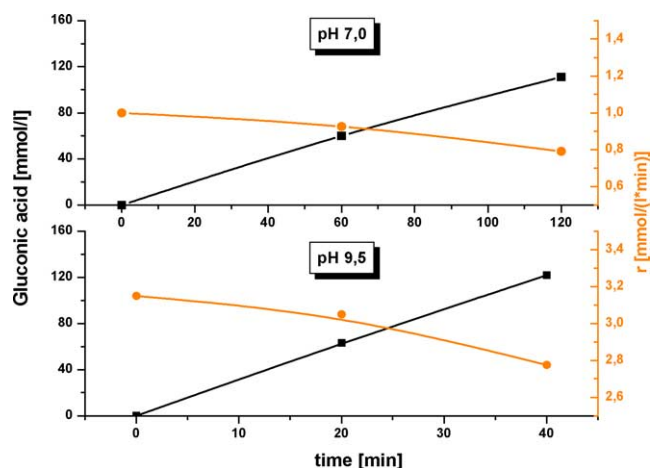


Fig. 10. Temporal concentration and reaction rate courses at pH 7.0 and 9.5 and $T = 50^\circ\text{C}$. Catalyst: Au/C GP3759 THPC.

early stages of the reaction deactivation of catalyst should not yet occur. According to Fig. 10, the initial reaction rates differ significantly ($3.15\text{ mmol L}^{-1}\text{ min}^{-1}$ at pH 9.5 vs $1.00\text{ mmol L}^{-1}\text{ min}^{-1}$ at pH 7.0). These data indicate that higher pH values obviously also favor the adsorption of D-glucose on the catalyst surface or the surface reaction.

4.2. Effect of Au particle size on catalyst activity

Although the intent was to prepare Au/C catalysts with the same metal loading (1 wt%), the values of Au content analyzed by ICP-OES differed widely (0.42–0.70 wt%). As a result the structure sensitivity of glucose oxidation over Au could not be reliably correlated with the mean particle size of the metal without considering Au loading. Thus, the effect of Au particle diameter on the activity of the catalyst was stud-

ied by calculating specific Au surfaces and correlating them with the initial reaction rates. A significant dependence of catalyst activity in the oxidation of D-glucose in the aqueous phase on specific Au surface area and, hence, Au particle diameter could be shown (see Fig. 5). Such a dependence can usually be related to differences in the adsorption behavior of the reactant on different crystal sites. As the metal particle size decreases, the relative proportions of surface atoms on corners and edges increase, implying the adsorption/hydrogenation of D-glucose, probably via the carbonyl group, on these highly exposed sites. Indeed, the latter were identified as active sites for the gold-catalyzed hydrogenation of the C=O bond of unsaturated aldehydes [20].

Although the observed rate enhancement of glucose oxidation with increasing specific Au surface area (i.e., reduction of particle size) is the expected sympathetic behavior, it has to be noted that structure sensitivity can be caused by a cooperative effect of particle size, degree of rounding, and portion of multiple-twinned particles as shown by our group in a recent study with oxide-supported gold catalysts [21]. To elucidate structure sensitivity in terms of gold particle morphology, high-resolution transmission electron microscopy should be involved in further studies.

Furthermore, it is important to mention that in this study, focusing only on the particle size effect, different kinds of support materials and reducing agents (THPC and NaBH_4) were used to prepare gold catalysts with various Au particle diameters; the trends were reported in Section 3.1. In principle, the generation of particle size itself can be influenced by the type of support and the reducing agent. However, from the rates of D-gluconic acid formation, using the catalysts Au/C GP3759 PVA and Au/C GP3759 THPC, we observed that gold particles with diameters of 3.7 nm ($A_{\text{spec}} = 84.0\text{ m}^2/\text{g}$) and 3.3 nm ($A_{\text{spec}} = 94.2\text{ m}^2/\text{g}$) (see

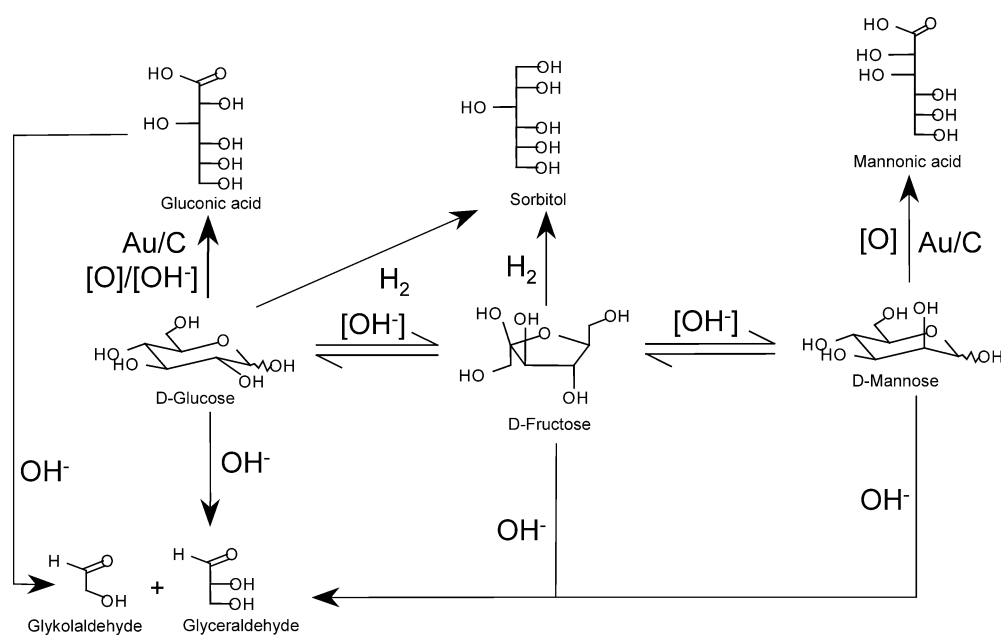


Fig. 11. Reaction network of the heterogeneously catalyzed D-glucose oxidation reaction in alkaline solution and at higher temperatures.

Fig. 1 and Table 3) gave rise to different activities (see Fig. 5) depending on the reducing agent (NaBH_4 vs THPC) but not on the support (Vulcan, which was identical in both cases). Nevertheless, for a more reliable examination of particle size effect, one should use the same support material and the same reducing agent and prepare the catalysts under different preparation conditions. This could be achieved, e.g., by variation of the concentration of the reducing agent or, as shown recently by us [21], by variation of pretreatment time and temperatures, leading to variation in Au particle size; however, this can be accompanied by a change in particle morphology.

Note also that each carbon support itself seems to affect differently the reactivity of the same gold particle size, indicating a specific metal–support interaction as shown for the liquid-phase oxidation of ethylene glycol by a combination of XPS and activity data of catalysts differing only in carbon support [22]. From XPS investigation of the gold catalysts in our study, the atomic Au/C ratios, based on corrected intensities of the Au $4f_{7/2}$ and C $1s$ signals, were calculated. However, regardless of the pretreatment procedure (as prepared or heated in argon or hydrogen at 350°C), the average ratio was considerably higher for gold supported on Vulcan-type carbon, $(6.2 \pm 1.0) \times 10^{-4}$, than for gold on Black Pearls, $(3.5 \pm 0.3) \times 10^{-4}$, indicating primarily a higher gold dispersion of the former according to the TEM results ($d_{\text{Au}} = 3.3$ and 3.7 nm for Au on Vulcan vs $d_{\text{Au}} = 5.0$ and 6.1 nm for Au on Black Pearls).

4.3. Reaction network of D-glucose oxidation

The selectivity of the liquid-phase oxidation of D-glucose as a polyfunctional molecule to D-gluconic acid depends greatly on the correct choice of reaction conditions. If the reaction temperature and pH are too high ($T > 70^\circ\text{C}$, $\text{pH} > 9$), a number of side reactions of D-glucose, presented in Fig. 11, have to be considered. In experiments carried out at higher pH values (> 7.0), formation of fructose occurred at any temperature. Formation of mannose occurred only at higher temperatures ($> 70^\circ\text{C}$) and higher pH values (> 9.0). D-Glucose as well as its isomerization products are not stable

at higher reaction temperatures and pH values and reacts further, as shown by our HPLC analysis, mainly to glycolaldehyde, glyceraldehyde, and dihydroxyacetone. These reaction pathways are probably a kind of retro-aldol reaction. To our knowledge, in this study the formation of sorbitol, a well-known reaction product of the hydrogenation of glucose over precious metal catalysts [12], has been reported as another side reaction in D-glucose oxidation at higher temperatures and pH values, for the first time. This phenomenon is important evidence of the oxidative dehydrogenation mechanism already mentioned in Section 3.4.2 which is passed in the formation of gluconic acid. According to the reaction mechanism of aldehyde oxidation to acids already proposed [16], the following reaction steps should be considered, and are presented in Fig. 12. In the aqueous phase, D-glucose exists in the pyranose form with 99.9% and in the open chain structure with 0.1%. The open-chain D-glucose converts in aqueous solution into the hydrate which should be stable because D-glucose is a very instable aldehyde. After adsorption on the catalyst surface, the hydrate is dehydrogenated and eventually desorbed. The desorption of gluconic acid is thereby faster if the substrate is deprotonated ($\text{pH} > 7.0$); otherwise catalyst deactivation by self-poisoning cannot be neglected. Another reason for the pH dependence of reaction rate is formation of the hydrate, which is faster in weakly alkaline or acidic media. Because in acidic media, the overall reaction rate should be limited by desorption of D-gluconic acid, a weakly alkaline solution should be preferred. Hydrides bound to the surface react with adsorbed OH_{ad} to form water, which is also desorbed.

The reaction rate of sorbitol formation correlates with the catalytic activity concerning D-glucose oxidation which is an important hint for the above-postulated reaction mechanism. The formation of sorbitol can be explained by a partially hydride-covered catalyst surface as an immediate consequence of the oxidative dehydrogenation mechanism. Because the degree of hydride coverage should correlate with the catalytic activity concerning D-glucose oxidation, it is not surprising that the reaction rate of sorbitol formation correlates with the reaction rate of D-gluconic acid formation. The formation of sorbitol can certainly not be explained

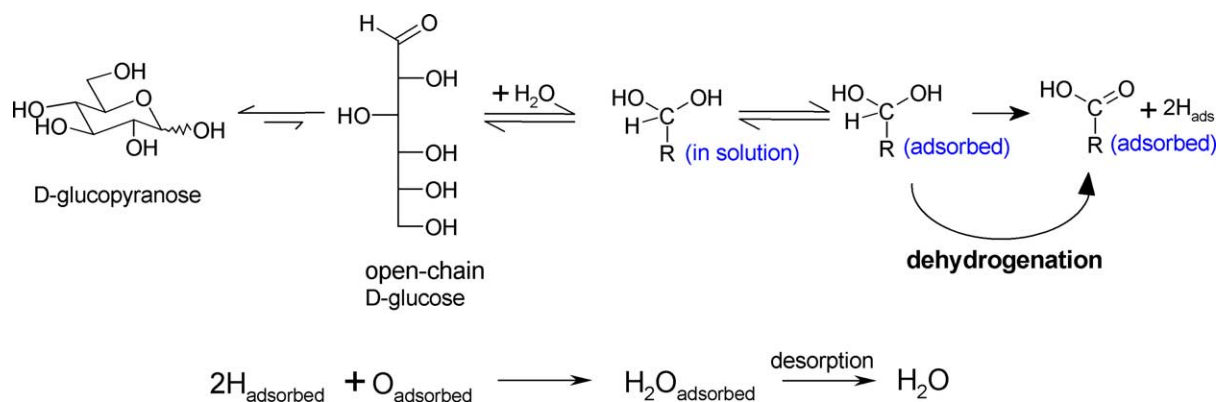


Fig. 12. Simplified reaction mechanism of the heterogeneously catalyzed D-glucose oxidation.

by a Cannizzaro-like side reaction of D-glucose in solution, because only aldehydes without hydrogen in α -position are subject to the Cannizzaro reaction in strongly alkaline solution.

4.4. Kinetic model

First, it was proved that the kinetic experiments were performed under reaction conditions (sufficient stirring rate, airflow rate) at which by external mass transfer at the phase boundaries does not limit the overall reaction rate. Then the rate-determining step according to the Langmuir–Hinshelwood model was indicated by studying the influence of different catalyst concentrations and initial D-glucose concentrations on the reaction rate of D-glucose oxidation. Although the reaction rate correlates with catalyst concentration, the rate-determining step of the heterogeneously catalyzed reaction cannot be stated, as all elementary steps according to the Langmuir–Hinshelwood model (adsorption, surface reaction, and desorption) can be influenced by catalyst concentration. In another series of experiments, it could be shown that the reaction rate does not significantly change at different initial D-glucose concentrations. Therefore, it could be proved that adsorption of the substrate on the catalyst surface is certainly not the rate-determining step. A detailed differentiation, by experiments, of whether the surface reaction or the desorption of D-gluconic acid is the rate-determining step has not been carried out yet. Because at lower pH values (< 7.0) the catalyst is deactivated by self-poisoning [17], desorption of D-gluconic acid should certainly not be a rate-limiting factor, if the reaction is run in an alkaline medium as it was in our kinetic experiments. The overall reaction rate should therefore be limited by the surface reaction and can be described by the semiempirical model according to Eqs. (3) and (4). Thus, it was assumed that the equilibrium of the surface reaction is widely on the product side.

To check the reliability of the kinetic parameters determined, the latter were varied and the resulting temporal concentration profiles of D-glucose were compared (Fig. 13). The degree of variation of the kinetic parameters was always the same, so that the effect of the parameters on the concentration profiles of D-glucose could be estimated more reliably. If the value of k_{Ox} is changed, the degree of deviation of the calculated concentration profiles will be very high. In particular, the slope of the concentration profile at the beginning of the reaction depends on k_{Ox} . Provided that this slope is accurately determined, the calculated value for k_{Ox} (k_1) should be credible.

If the sorption equilibrium constant K_G is varied, the change in the concentration profiles of D-glucose is less distinctive. If one wants to determine a reliable value for K_G , above all the transition areas of the concentration profiles of D-glucose and D-gluconic acid according to Fig. 14 have to be analyzed precisely by a large number of HPLC samples. In this transition area the D-glucose concentration has

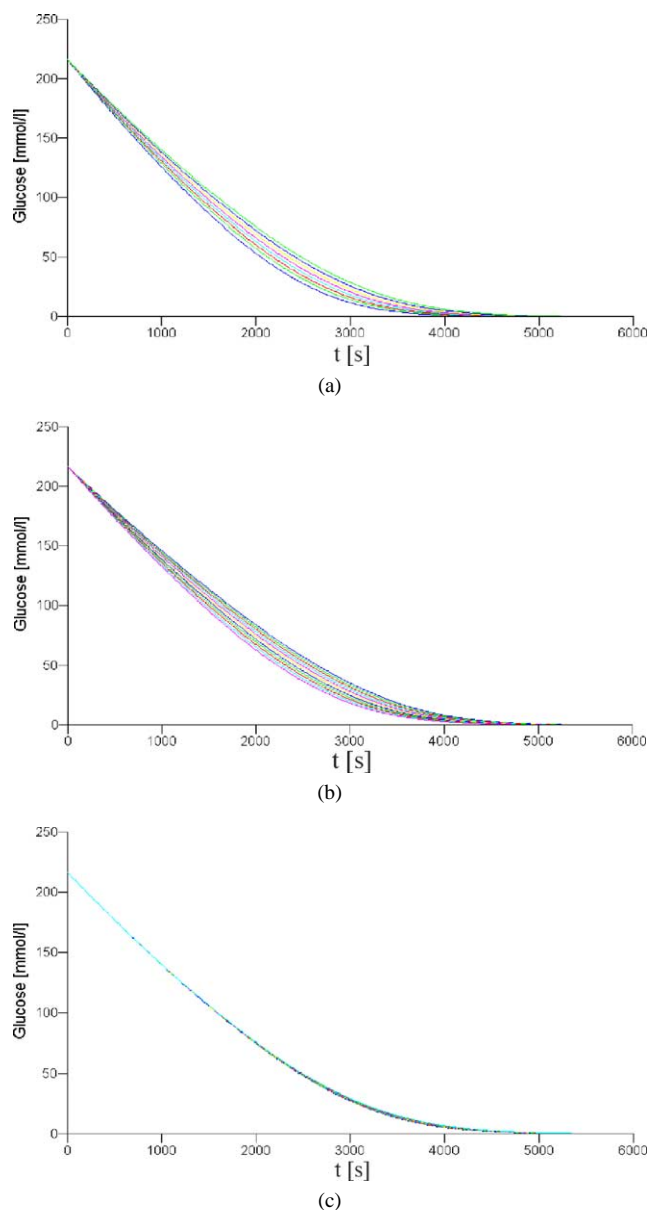


Fig. 13. Concentration courses of D-glucose at varied kinetic parameters: (a) $k_{\text{Ox}} = 63.3 \times 10^3$ – 77.9×10^3 ($k_1 = 13 \times 10^{-3}$ – 15×10^{-3}). (b) $K_G = 4 \times 10^5$ – 5×10^6 . (c) $K_{\text{GS}} = 67 \times 10^4$ – 76×10^4 .

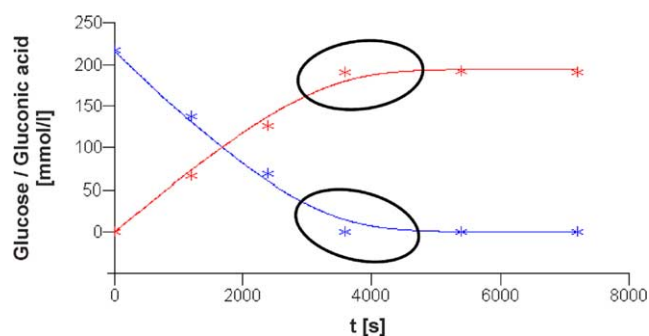


Fig. 14. Transition area (marked) of the concentration courses of D-glucose and D-gluconic acid.

already decreased to a small value, and the catalyst surface should not be covered completely with D-glucose. Thus, the adsorption of D-glucose is the rate-determining step of the reaction and a modeling that represents this transition area correctly should provide a reliable value for K_G .

The concentration profiles of D-glucose hardly change, when the value of K_{GS} is varied. That means that the desorption of D-gluconic acid is always very fast compared with the rates of the other elementary steps, so that the overall reaction rate is never affected by this step.

To check the optimization routine, initial values for the kinetic parameters were varied widely and their influence on the calculated parameters was analyzed. The resulting concentration courses were all in good agreement with the experimental data. It is notable that the adsorption constant of D-gluconic acid was always smaller than that of D-glucose. Furthermore, the values calculated for k_1 were always similar independent of the model applied.

5. Conclusions

This investigation highlights the following points:

- (i) Nanosized gold particles in the range of 3–6 nm prepared on Black Pearls and Vulcan-type carbons are active in liquid-phase oxidation of D-glucose to gluconic acid. The most active gold catalyst had a specific gold surface area of $94.2 \text{ m}^2/\text{g}$.
- (ii) Reaction conditions could be optimized with respect to the reaction rate of D-gluconic acid formation and the selectivity of the reaction. The best results were obtained at 50°C and pH 9.5. Reasons for the effect of temperature and pH on reaction rate of D-gluconic acid formation were proposed, and on the basis of these arguments together with the carefully estimated analysis of reaction products, a reaction network was presented. The reaction could be successfully described by an oxidative dehydrogenation mechanism in the aqueous phase which could be confirmed by experimental observations.
- (iii) It could also be shown that D-glucose oxidation is a structure-sensitive reaction as a significant increase in reaction rate could be observed with increasing Au specific surface area under the same reaction conditions.
- (iv) Kinetic runs were carried out neglecting mass transfer at the phase boundaries by intensive stirring and high volumetric flow rate of air. By analyzing the effect of catalyst concentration, initial D-glucose concentration, and pH value of the liquid phase on reaction rate, it could be shown that the surface reaction is the rate-limiting step according to a semiempirical model based on a Langmuir–Hinshelwood-type pathway. On the basis of these results, kinetic parameters were calculated for the first time by an optimization routine and the reliability of the determined parameters was checked by different methods.

Acknowledgments

The authors thank Dr. C. Mohr for the TEM analysis of the catalysts at the Max-Planck-Institute for Microstructure Physics Halle, and Dr. J. Radnik (Institute for Applied Chemistry Berlin) for the XPS measurements.

Appendix A. Nomenclature

$[G]_L/[GS]_L$	D-Glucose/D-gluconic acid concentration;
$[G]_S/[GS]_S$	D-Glucose/D-gluconic acid concentration on the catalyst surface;
$k_{\text{ads,G}}/k_{\text{des,G}}$	Adsorption/desorption constant of D-glucose;
k_1/k_{-1}	Reaction rate constants of the surface reaction;
$k_{\text{des,GS}}/k_{\text{ads,GS}}$	Desorption/adsorption constant of D-gluconic acid;
k_P	Empirical reaction constant of side reactions of D-glucose;
θ_G	D-Glucose coverage grade of catalyst surface;
θ_{GS}	D-Gluconic acid coverage grade of catalyst surface;
r_{surface}	Reaction rate of surface reaction;
r_{OR}	Overall reaction rate;
$r_{\text{Sor,G}}$	Rate of D-glucose sorption;
$r_{\text{Sor,GS}}$	Rate of D-gluconic acid sorption;
M_C	Catalyst concentration;
X	Conversion of D-glucose;
S	Selectivity to D-gluconic acid.

References

- [1] Ullmanns Encyclopedia of Industrial Chemistry, Electronic Release, Wiley–VCH, 2003; http://www.mrw.interscience.wiley.com/ueic/articles/a12_449/frame.html.
- [2] F.W. Lichtenthaler, Acc. Chem. Res. 35 (2002) 728–737.
- [3] M. Besson, P. Gallezot, in: R.A. Sheldon, H. van Bekkum (Eds.), Fine Chemicals through Heterogeneous Catalysis, Wiley–VCH, 2001, pp. 509–510, Chap. 9.3.
- [4] M. Besson, P. Gallezot, Catal. Today 81 (2003) 547–559.
- [5] S. Biella, L. Prati, M. Rossi, J. Catal. 206 (2002) 242–247.
- [6] A. Martin, H. Berndt, I. Pitsch, A. Dittmar, in: Proceedings of 7th European Workshop on Selective Oxidation, EuropaCat VI, Innsbruck, Austria, September 1–2, 2003; <http://www.icp.csic.es/iso2003/Programme%20ISO03.doc>.
- [7] S. Biella, G.L. Castiglioni, C. Fumagalli, L. Prati, M. Rossi, Catal. Today 72 (2002) 43–49.
- [8] F. Porta, L. Prati, M. Rossi, S. Coluccia, G. Martra, Catal. Today 61 (2000) 165–172.
- [9] C. Bianchi, F. Porta, L. Prati, M. Rossi, Top. Catal. 13 (2000) 231–233.
- [10] J.D. Grunwaldt, C. Kiener, C. Wögerbauer, A. Baiker, J. Catal. 181 (1999) 223–232.
- [11] P. Claus, S. Schimpf, Y. Önal, in: Proceedings of 18th North American Catalysis Society Meeting, Cancun, Mexico, June 1–6, 2003, p. 365.
- [12] B. Kusserow, S. Schimpf, P. Claus, Adv. Synth. Catal. 345 (2003) 1–11.
- [13] J. Radnik, C. Mohr, P. Claus, Phys. Chem. Chem. Phys. 5 (2003) 172–177.
- [14] NIST database for XP spectroscopy; <http://srdata.nist.gov/xps>.
- [15] J.M. Montejano-Carrizales, F. Aguilera-Granja, J.L. Moran-Lopez, Nanostruct. Mater. 8 (1997) 269–287.

- [16] T. Mallat, A. Baiker, *Catal. Today* 19 (1994) 247–284.
- [17] M. Besson, P. Gallezot, *Catal. Today* 57 (2000) 127–141.
- [18] I. Nikov, K. Paev, *Catal. Today* 24 (1995) 41–47.
- [19] (a) W. Reschetilowski, in: *Technisch-Chemisches Praktikum*, Wiley–VCH, 2002, pp. 116, 117;
(b) *Perry's Chemical Engineers' Handbook*, McGraw–Hill, New York, 1999, pp. 2-217, 2-125.
- [20] C. Mohr, H. Hofmeister, J. Radnik, P. Claus, *J. Am. Chem. Soc.* 125 (2003) 1905–1911.
- [21] C. Mohr, H. Hofmeister, P. Claus, *J. Catal.* 213 (2003) 86–94.
- [22] C.L. Bianchi, S. Biella, A. Gervasini, L. Prati, M. Rossi, *Catal. Lett.* 85 (2003) 91–96.
- [23] D. Pantea, H. Darmstadt, S. Kaliaguine, Ch. Roy, *Appl. Surf. Sci.* 217 (2003) 181–193.